Optimal control strategies based on extended Kalman filter in mathematical models of COVID-19

Dewi Suhika[1,2], Roberd Saragih[1], Dewi Handayani[1], Mochamad Apri[1]
[1]Department of Mathematics, Faculty of Mathematics and Natural Sciences, Institut Teknologi Bandung, Bandung, Indonesia
[2]Department of Mathematics, Faculty of Sciences, Institut Teknologi Sumatera, Bandar Lampung, Indonesia

Article Info	ABSTRACT
	The Omicron variant of the severe acute respiratory syndrome coronavirus 2 (SARS-CoV-2) virus is an extremely contagious variant that has garnered global attention due to its potential for rapid spread and its impact on the effectiveness of vaccines and non-pharmacological measures. In this paper, we investigate mathematical models involving vaccinated individuals and control functions to analyze how the spread of coronavirus disease 2019 (COVID-19) infection evolves over time. In the process of constructing a mathematical model for COVID-19, there are many parameters whose values are not yet known with certainty. Therefore, the extended Kalman filter method is used as a tool to estimate these parameters in an effort to better understand the dynamics of the spread and evolution of this disease. This method helps align the mathematical model with existing empirical data, allowing us to make more accurate predictions about the course of the COVID-19 pandemic and plan more precise actions to address the situation. Furthermore, an optimal control design is applied to reduce the number of infected individuals by implementing seven strategies involving a combination of health education, vaccination, and isolation controls. The simulation results we conducted indicate that the use of optimal control strategies can lead to a significant decrease in the number of individuals infected with COVID-19.

Corresponding Author:

Dewi Suhika
Department of Mathematics, Faculty of Mathematics and Natural Sciences, Institut Teknologi Bandung
Bandung, Indonesia
Email: 30120006@mahasiswa.itb.ac.id

1. INTRODUCTION

Coronavirus disease 2019 (COVID-19) first detected in Wuhan, China at the end of 2019 [1], has rapidly evolved into a global pandemic, disrupting nearly all aspects of life. As the virus spread worldwide, it underwent several mutations leading to the emergence of variants such as Alpha (B.1.1.7), first identified in the United Kingdom on December 18, 2020, which has several mutations in the viral spike protein enhancing its ability to attach to human cells and increasing transmission [2]. Following the Alpha variant, the Beta variant (B.1.351) was reported in South Africa in December 2020, featuring mutations that could potentially impact vaccine and antibody efficacy [3]. Similarly, the Gamma variant (P.1) was identified in Brazil on January 21, 2021, and the Delta variant (B.1.617.2), known for being more contagious than its predecessors, raised global concerns in April 2021 [4]. The latest, the Omicron variant (B.1.1.529), was first reported in South Africa on November 24, 2021 [5], and has quickly become a major concern due to its numerous mutations, some previously unseen, which contribute to its faster transmission rate and potential to overcome existing immunity [6]. These variants have not only increased the complexity of controlling the virus's spread

but also challenged the effectiveness of established public health strategies. In Indonesia, the swift predominance of the Omicron variant since late 2021 has exacerbated strains on an already overwhelmed national health system and complicated ongoing vaccination efforts [7].

Mathematical models are crucial tools for understanding and managing the spread of the COVID-19 virus. Research using mathematical models has been conducted extensively since the pandemic began. These models are used to understand virus transmission, predict epidemiological trends, plan interventions, and make policy decisions [8]. Research by Annas *et al.* [9] developed an susceptible–exposed–infectious–removed (SEIR) model that incorporated vaccination and isolation parameters, providing insights into the effectiveness of these interventions in slowing the spread. Another study by Wang *et al.* [10] adapted the SEIR model to include compartments for susceptible (S), exposed (E), infected (I), hospitalized (H), and removed (R), using public data from Wuhan. This model was utilized to determine the initial date of COVID-19 infection in Wuhan, considering the lack of information on initial conditions. Sun *et al.* [11] constructed the SEIR model with an added quarantine (Q) compartment to assess the impact of lockdown measures and the availability of medical resources in Wuhan during 2020 on the virus's dynamics and spread. The results indicated that the longer the lockdown was implemented in Wuhan, the fewer people were infected, but this had implications for other cities in China and around the world. However, despite these advancements, current models often struggle to adapt to the rapidly evolving dynamics of the virus, especially with the frequent emergence of new variants. There is a pressing need for models that incorporate real-time data, which could significantly improve the accuracy of predictions and the effectiveness of interventions.

The concept of optimal control is particularly relevant in managing dynamic systems like pandemics, where it aims to identify the most effective strategies under given constraints [12]. Many researchers have utilized optimal control theory to address infectious disease control issues. Madubueze *et al.* [13] investigates optimal control in COVID-19 models as non-pharmacological strategies such as quarantine and isolation. Sweilam *et al.* [14] explores optimal control as medical treatment strategies such as isolation in healthcare facilities and the provision of respiratory aids, involving variations in parameters related to contact rates and infection transmission. Djidjou-Demasse *et al.* [15] utilizes optimal control theory to explore the best strategy that can be implemented while awaiting the vaccine by seeking a solution that minimizes the number of deaths and the costs resulting from the implementation of the control strategy itself. Their findings show that such a solution leads to an increasing level of control peaking around the 16th month from the onset of the epidemic, followed by a steady decline until the vaccine is implemented. Li and Guo [4] employed optimal control by implementing a vaccination control strategy in a model with COVID-19 mutations (Delta strain). However, existing models have not specifically addressed the challenges posed by the Omicron variant and the original virus, nor have they fully utilized the potential of real-time data integration from both aspects.

This study aims to address these limitations by enhancing the responsiveness of the SEIR model to changes in virus transmission dynamics through the integration of the extended Kalman filter and optimal control strategies. This approach is designed to not only improve the adaptability of our models but also to provide more effective and timely responses to the pandemic's challenges. Specifically, we focus on the application of these advanced techniques to manage populations that have been vaccinated, aiming to refine the control strategies against COVID-19 more effectively.

The next part of this paper will describe the methodology we use, including details about the integration of the extended Kalman filter and the development of optimal control strategies. We will present simulation results to demonstrate the effectiveness of this approach in reducing the spread of COVID-19. Subsequently, the discussion will critique these results in the context of existing literature and their impact on public health policy. The conclusion will summarize the significant findings and propose directions for future research in this field.

2.   METHOD

In constructing a mathematical model, appropriate assumptions are needed to make the model simpler, easier to analyze, understand, and implement. Furthermore, one of the important challenges in mathematical models is determining parameter values based on data, requiring optimization methods to overcome this difficulty. In this paper, we applied the extended Kalman filter and succeeded in estimating the values of several previously unknown parameters. Additionally, we developed control strategies to effectively manage the spread of the disease. The results of these control strategies are simulated to demonstrate their effectiveness in controlling the outbreak. The research methodology is illustrated in Figure 1.

2.1. Data collection

In this study, COVID-19 data collection was carried out by obtaining daily data from the Health Department for the period from February 6 to May 5, 2022, specifically for the DKI Jakarta province. The collected data includes the number of new cases, active cases, vaccinations, quarantines, recoveries, and

deaths that occurred each day during the period. The use of this data aims to analyze the trends in virus spread, the effectiveness of the interventions applied, and the dynamics of case changes in the community. This information is crucial for understanding the characteristics of COVID-19 spread in the region and serves as a basis for further health policy decisions.
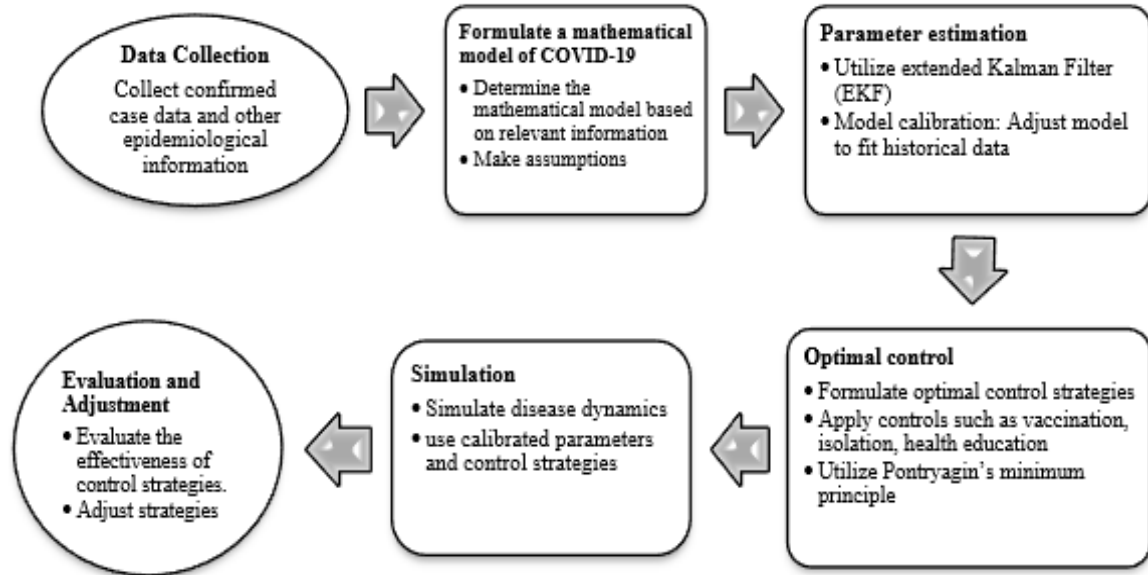

Figure 1. Research process diagram for the optimization of the mathematical model of COVID-19

2.2. Formulate a mathematical model of COVID-19

In this paper, the model employed is provided with assumptions as problem constraints to facilitate the construction of the model. The assumptions utilized are i) The average birth rate is equal to the average death rate, so the total population is constant; ii) The population is closed. There is no movement (migration, mobility) to or from the observed area; iii) Every human being born enters a susceptible population; iv) Individuals who have received the vaccine but have not yet generated antibodies might still be susceptible to infection. When the vaccine does not offer full immunity against the virus, vaccinated individuals can remain at risk of contracting the disease [16]; v) Infection with the Omicron variant is transmitted through contact with individuals carrying this variant, whereas infection with the original strains occurs via contact with individuals infected with those strains. It is important to note that susceptible individuals who come into contact with those infected with the original virus may contract that virus but will not become infected with the Omicron variant unless exposed to it specifically [17]; vi) Transmission occurs through interactions between susceptible and infected individuals [18]; and vii) Individuals who are recorded as confirmed positive if declared cured are assumed to be immune to COVID-19.

2.3. Parameter estimation

Extended Kalman filter (EKF) is an algorithm designed to estimate states in nonlinear dynamic systems and is represented by (1).

$$dx(t) = f\big(x(t)\big)dt \tag{1}$$

where $f(.)$ denotes the nonlinear system function. By discretizing (1) in time domain, we can obtain the discrete-time model:

$$x_{k+1} = x_k + f(x_k) \tag{2}$$

where x_k represents the system state at time point k.

The steps of the extended Kalman filter algorithm proceed as follows, after converting (1) into its discrete form.

a. Linearize the system model (1), resulting in the Jacobian matrix A.
b. Initialization of each state variable and parameter when $k = 0$ for the system model (1).
c. Determine the initial value of the error covariance $\hat{P}_0$ based on [19].

$$\hat{P}_0 = E[(x_0 - \hat{x}_0)(x_0 - \hat{x}_0)^T]$$

d. Calculate the predicted state using

$$\hat{x}_k^- = A\hat{x}_{k-1}.$$

e. Determine the error covariance value obtained using the equation,

$$P_k^- = AP_{k-1}A^T + \mathbb{Q}_k$$

f. Next is the correction stage. Calculate Kalman gain based on the following equation,

$$K_k = P_k C^T (CP_k^- C^T + \mathcal{R}_k)^{-1},$$

with C is the observation matrix.

g. Update state estimates based on the following equation,

$$\hat{x}_k = \hat{x}_k^- + K_k(z_k - C\hat{x}_k^-)$$

h. Calculate the error covariance using the following equation,

$$P_k = [I - K_k C]P_k^-$$

Repeat steps (a)-(d) until all iterations are processed and the values converge.

2.4. Optimal control

Numerically solving this optimal control problem utilizing Pontryagin's minimum principle involves developing an algorithm to generate an approximate optimal control solution. The optimal system encompasses state equations, along with their initial conditions, costate equations, and associated transversality conditions, as well as optimal control characteristics. This control problem can be solved using the backward-forward sweep algorithm as in [12], [20], in the following manner:

a. Divide the time interval $[0, T]$ into $\mathcal{N}$ equally spaced subintervals. Create vectors $x = (x_1, x_2, \ldots, x_6)$ and $\lambda = (\lambda_1, \lambda_2, \ldots, \lambda_6)$ to approximate the state and costate variables.
b. Initialize the values of φ_1, φ_2, and φ_3 for the entire time interval, setting $\varphi_1(0) = \varphi_2(0) = \varphi_3(0) = 0$. The vectors φ_1, φ_2, and φ_3 represent control approximations at time t.
c. Starting with the initial condition $x_1 = x(t_0) = x_0$ and the values in φ_1, φ_2, and φ_3, state differential equation is solved forward with respect to time using the 4th order Runge-Kutta method. This provides a numerical estimate for the state development.
d. Using the transversality condition $\lambda_{\mathcal{N}+1} = \lambda(T) = 0$ and the vector values $\varphi_1, \varphi_2, \varphi_3$, and x, solve the costate equation backward in time using the 4th-order Runge-Kutta method. This provides a numerical estimate for the costate.
e. The control values φ_1, φ_2, and φ_3 are updated by substituting the state and costate values into the optimal control characterization.
f. Next, a convergence check is carried out. If the value of the variable being calculated in the current iteration and the value in the previous iteration are quite close or converge, then the value of the variable in the current iteration is considered an acceptable solution. This indicates that the algorithm has converged or is approaching the optimal solution. If not, the algorithm returns to step 2 for the next iteration.

This process is repeated iteratively until the numerical solution converges to the optimal solution of the given optimal control problem. This method is a combination of forward and backward approaches to find optimal control using the 4th order Runge-Kutta numerical method. The forward approach involves simulating the state dynamics forward in time using initial guesses for the control variables, while the backward approach involves adjusting these control variables based on the discrepancies observed in the

desired state trajectory. Through iterative refinement of controls, this method efficiently addresses the challenges of non-linearities and constraints in control systems, ensuring accuracy and stability in the computed solutions.

3.   RESULTS AND DISCUSSION
3.1.   Result of the COVID-19 model
In the COVID-19 model, the population $N(t)$ is categorized into eight distinct compartments to better understand and simulate the spread of the virus and its variants. The compartment $S(t)$ represents the subpopulation of individuals who are susceptible to the virus and have not been vaccinated. $E_1(t)$ and $E_2(t)$ denote individuals who have been exposed to the original COVID-19 virus and the Omicron variant, respectively. $V(t)$ includes those who have received vaccinations. $I_1(t)$ and $I_2(t)$ are subsets of the population infected with the original virus and the Omicron variant, respectively. $H(t)$ refers to those who are severely infected and currently hospitalized, while $R(t)$ represents individuals who have recovered from the infection, highlighting the dynamics and interactions between different stages of the disease within the population. Thus, the total population is given by,

$$N(t) = S(t) + E_1(t) + E_2(t) + V(t) + I_1(t) + I_2(t) + H(t) + R(t)$$

The mathematical model for the spread of COVID-19 along with control input can be seen in the following system:

$$\dot{S}(t) = \Lambda - \frac{\beta_1 S I_1}{N}\big(1 - \varphi_1(t)\big) - \frac{\beta_2 S I_2}{N}\big(1 - \varphi_1(t)\big) - \big(1 + \varphi_2(t)\big)\sigma S - \mu S$$
$$\dot{E}_1(t) = \frac{\beta_1 S I_1}{N} + \frac{\beta_1 \omega_1 V I_1}{N} - \alpha_1 E_1 - \mu E_1$$
$$\dot{E}_2(t) = \frac{\beta_2 S I_2}{N} + \frac{\beta_2 \omega_2 V I_2}{N} - \alpha_2 E_2 - \mu E_2$$
$$\dot{V}(t) = \big(1 + \varphi_2(t)\big)\sigma S - \frac{\beta_1 \omega_1 V I_1}{N} - \frac{\beta_2 \omega_2 V I_2}{N} - \mu V$$
$$\dot{I}_1(t) = \alpha_1 E_1 - \varphi_3(t) I_1 - \gamma_1 I_1 - \mu I_1$$
$$\dot{I}_2(t) = \alpha_2 E_2 - \varphi_3(t) I_2 - \gamma_2 I_2 - \mu I_2$$
$$\dot{H}(t) = \varphi_3(t) I_1 + \varphi_3(t) I_2 - \gamma_3 H - \mu H$$
$$\dot{R}(t) = \gamma_1 I_1 + \gamma_2 I_2 + \gamma_3 H - \mu R \tag{3}$$

and the explanation of the parameters in model (3) are provided in Table 1.

The control variable $\varphi_1(t)$ represents health education provided to individual S with the aim of enhancing their understanding of personal health conditions, disease prevention efforts, and steps to maintain optimal health. The control variable $\varphi_2(t)$ represents the vaccination intervention, which is intended to mitigate and manage the transmission of COVID-19 by increasing the vaccination coverage among the population. The control variable $\varphi_3(t)$ is the isolation rate given to I_1 and I_2 with the aim of reducing the infected population of I_1 and I_2.

The basic reproduction number (R_0) is given by,

$$R_0 = max\left\{\frac{\left(\frac{\beta_1 \Lambda}{N(\sigma + \mu)} + \frac{\beta_1 \omega_1 \Lambda \sigma}{N(\sigma + \mu)\mu}\right)\alpha_1}{a_1}, \frac{\left(\frac{\beta_2 \Lambda}{N(\sigma + \mu)} + \frac{\beta_2 \omega_2 \Lambda \sigma}{N(\sigma + \mu)\mu}\right)\alpha_2}{a_3}\right\}.$$

Disease-free conditions occur if the disease is not endemic or infection has not occurred, namely when $R_0 < 1$. Endemic conditions occur if the disease is not endemic or infection has not occurred, namely when $R_0 > 1$.

3.2.   Result of parameter estimation using extended Kalman filter
Before estimating the COVID-19 spread model using the extended Kalman filter (EKF), discretization will be carried out first. Discretization itself aims to obtain the form of the equation in a discrete state [21]. This is because the EKF method is a system model that uses measurements and a discrete time system model. In the COVID-19 model (3), it will be discretized using a forward finite difference method for changes in variables over time. The following is a discretization of the COVID-19 disease transmission model:

$$S_{k+1} = S_k + \left(\Lambda - \frac{\beta_1 S_k I_{1_k}}{N} - \frac{\beta_2 S_k I_{2_k}}{N} - \sigma S_k - \mu S_k\right)\Delta t$$

$$E_{1_{k+1}} = E_{1_k} + \left(\frac{\beta_1 S_k I_{1_k}}{N} + \frac{\beta_1 \omega_1 V_k I_{1_k}}{N} - \alpha_1 E_{1_k} - \mu E_{1_k}\right)\Delta t$$

$$E_{2_{k+1}} = E_{2_k} + \left(\frac{\beta_2 S_k I_{2_k}}{N} + \frac{\beta_2 \omega_2 V_k I_{2_k}}{N} - \alpha_2 E_{2_k} - \mu E_{2_k}\right)\Delta t$$

$$V_{k+1} = V_k + \left(\sigma S_k - \frac{\beta_1 \omega_1 V_k I_k}{N} - \frac{\beta_2 \omega_2 V_k I_{2_k}}{N} - \mu V_k\right)\Delta t$$

$$I_{1_{k+1}} = I_{1_k} + \left(\alpha_1 E_{1_k} - \varphi_3 I_{1_k} - \gamma_1 I_{1_k} - \mu I_{1_k}\right)\Delta t$$

$$I_{2_{k+1}} = I_{2_k} + \left(\alpha_1 E_{2_k} - \varphi_3 I_{2_k} - \gamma_2 I_{2_k} - \mu I_{2_k}\right)\Delta t$$

$$H_{k+1} = H_k + \left(\varphi_2 I_{1_k} + \varphi_3 I_{2_k} - \gamma_3 H_k - \mu H_k\right)\Delta t$$

$$R_{k+1} = R_k + \left(\gamma_1 I_{1_k} + \gamma_2 I_{2_k} + \gamma_3 H_k - \mu R_k\right)\Delta t. \tag{4}$$

The discrete model (4) can be simplified into the form of a nonlinear function as:

$$x_{k+1} = x_k + f(x_k)$$

where x_k is the system state at time point k. In model (4) a new state variable, $\dot{\beta}_{1_k} = 0, \dot{\beta}_{2_k} = 0, \dot{\sigma}_k = 0,$ $\dot{\alpha}_{1_k} = 0, \dot{\alpha}_{2_k} = 0, \dot{\gamma}_{1_k} = 0, \dot{\gamma}_{2_k} = 0 \ \dot{\gamma}_{3_k} = 0$ dan $\dot{\varphi}_{3_k} = 0$. Next, to form a system model, in (4) a stochastic factor in the form of noise is added as:

$$S_{k+1} = S_k + \left(\Lambda - \frac{\beta_{1_k} S_k I_k}{N} - \frac{\beta_{2_k} S_k I_{2_k}}{N} - \sigma_k S_k - \mu S_k\right)\Delta t + w_{1_k}$$

$$E_{1_{k+1}} = E_{1_k} + \left(\frac{\beta_{1_k} S_k I_{1_k}}{N} + \frac{\beta_{1_k} \omega_1 V_k I_{1_k}}{N} - \alpha_{1_k} E_k - \mu E_k\right)\Delta t + +w_{2_k}$$

$$E_{2_{k+1}} = E_{2_k} + \left(\frac{\beta_{2_k} S_k I_{2_k}}{N} + \frac{\beta_{2_k} \omega_2 V_k I_{2_k}}{N} - \alpha_{2_k} E_{2_k} - \mu E_{2_k}\right)\Delta t + w_{3_k}$$

$$V_{k+1} = V_k + \left(\sigma_k S_k - \frac{\beta_{1_k} \omega_1 V_k I_k}{N} - \frac{\beta_{2_k} \omega_2 V_k I_{2_k}}{N} - \mu V_k\right)\Delta t + w_{4_k}$$

$$I_{1_{k+1}} = I_{1_k} + \left(\alpha_{1_k} E_{1_k} - \varphi_{3_k} I_{1_k} - \gamma_{1_k} I_{1_k} - \mu I_{1_k}\right)\Delta t + w_{5_k}$$

$$I_{2_{k+1}} = I_{2_k} + \left(\alpha_1 E_{2_k} - \varphi_{3_k} I_{2_k} - \gamma_{2_k} I_{2_k} - \mu I_{2_k}\right)\Delta t + w_{6_k}$$

$$H_{k+1} = H_k + \left(\varphi_{3_k} I_{1_k} + \varphi_{3_k} I_{2_k} - \gamma_{3_k} H_k - \mu H_k\right)\Delta t + w_{7_k}$$

$$R_{k+1} = R_k + \left(\gamma_{1_k} I_{1_k} + \gamma_{2_k} I_{2_k} + \gamma_{3_k} H_k - \mu R_k\right)\Delta t + w_{8_k}$$

$$\beta_{1_{k+1}} = \beta_{1_k} + w_{9_k}$$

$$\beta_{2_{k+1}} = \beta_{2_k} + w_{10_k}$$

$$\sigma_{k+1} = \sigma_k + w_{11_k}$$

$$\alpha_{1_{k+1}} = \alpha_{1_k} + w_{12_k}$$

$$\alpha_{2_{k+1}} = \alpha_{2_k} + w_{13_k}$$

$$\gamma_{1_{k+1}} = \gamma_{1_k} + w_{14_k}$$

$$\gamma_{2_{k+1}} = \gamma_{2_k} + w_{15_k}$$

$$\gamma_{3_{k+1}} = \gamma_{3_k} + w_{16_k}$$

$$\varphi_{3_{k+1}} = \varphi_{3_k} + w_{17_k} \tag{5}$$

where Δt is the change in time with $\Delta t = 0.01$. w_k is system noise in a system model that is normally distributed with zero mean and covariance $\mathbb{Q}_k$ or can be written $w_k \sim N(0, \mathbb{Q}_k)$.

It is assumed that the parameters to be estimated are: $\beta_{1_k}, \beta_{2_k}, \sigma_k, \alpha_{1_k}, \alpha_{2_k}, \gamma_{1_k}, \gamma_{2_k}, \gamma_{2_k}, \gamma_{3_k},$ and φ_{3_k} as a continuous piecewise functions with jumps every day, obtained in one day the values $\beta_{1_k}, \beta_{2_k}, \sigma_k, \alpha_{1_k}, \alpha_{2_k}, \gamma_{1_k}, \gamma_{2_k}, \gamma_{2_k}, \gamma_{3_k},$ and φ_{3_k} are constant, so that equations $\beta_{1_{k+1}} = \beta_{1_k}, \beta_{2_{k+1}} = \beta_{2_k}, \sigma_{k+1} = \sigma_k, \alpha_{1_{k+1}} = \alpha_{1_k}, \alpha_{2_{k+1}} = \alpha_{2_k}, \gamma_{1_{k+1}} = \gamma_{1_k}, \gamma_{2_{k+1}} = \gamma_{2_k}, \gamma_{3_{k+1}} = \gamma_{3_k},$ and $\varphi_{3_{k+1}} = \varphi_{3_k}$ satisfies. In the process of parameter estimation with extended Kalman filter, it is a common practice to introduce additional parameters as new state variables. Equation (5) is a system model, while the measurement model is:

$$z_k = C x_k + v_k$$

where v_k is the system noise in the measurement model which is normally distributed with zero mean and covariance $\mathcal{R}_k$ or usually written $v_k \sim N(0, \mathcal{R}_k)$.

The C matrix follows the available data which includes $S, E_1, E_2, V, I_1, I_2, Q,$ and R. The stochastic factor in the form of noise contained in the equation is generated from a number of random numbers from the computer through the MATLAB program. The noise generated is assumed to have a normal distribution with a mean of zero while the noise variance is assumed to be constant at $\mathbb{Q}_k$ and $\mathcal{R}_k$. By following the algorithm steps in sub section 2.3, estimation results are obtained which can be seen in Table 1. Validating the constructed model's accuracy entails comparing numerical simulation outcomes with actual data obtained from the DKI Jakarta Health Service from February 05 to May 05, 2022. The following is a graph comparing the infected population from the results of the numerical simulation with the data shown in Figure 2.

Table 1. Estimation results of several parameters with the extended Kalman filter (EKF)

| Parameter	Description	Result EKF	References
β_1	Transmission rate of the original virus	0.09717	Estimation
β_2	Transmission rate of the omicron virus	0.1097	Estimation
α	Vaccination rates	0.1053	Estimation
ω_1	Antibodies may not have been formed by vaccine recipients against the original virus after 28 days.	0.05	[17]
ω_2	Antibodies may not have formed in vaccine recipients against the Omicron virus after 28 days.	0.33	[22]
σ_1	The rate of change of individual exposures from E_1 to I_1	0.1052	Estimation
σ_2	The rate of change of individual exposures E_2 to I_2	0.1053	Estimation
γ_1	Recovery rate of each compartment I_1	0.04659	Estimation
γ_2	Recovery rate of each compartment I_2	0.05587	Estimation
γ_3	Recovery rate of each compartment Q	0.05134	Estimation
φ_3	isolation rate	0.659	Estimation
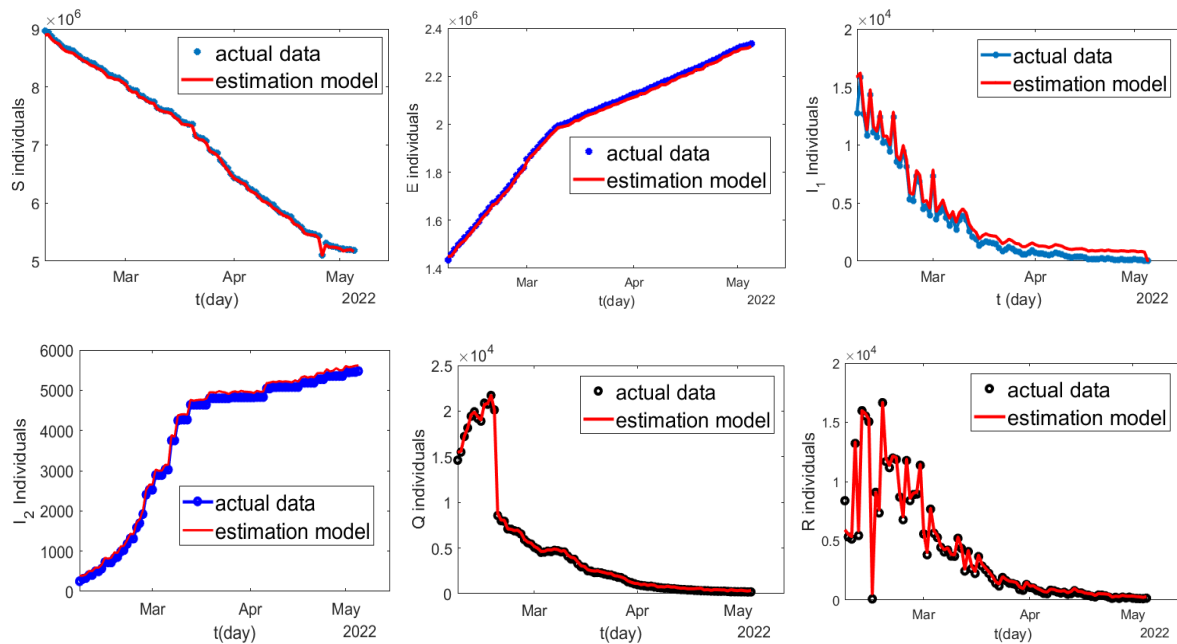
Figure 2. COVID-19 model simulation matching graph with real data

3.3. Design optimal control

In this subsection, we will be applying optimal control techniques to the COVID-19 model (3). The objective of this optimal control is to minimize the performance index with the goal of reducing the populations $I_1(t)$ and $I_2(t)$, which is formulated as (6),

$$J(\varphi_1, \varphi_2, \varphi_3) = \int_0^T \left(I_1(t) + I_2(t) + \frac{1}{2} B_1 \varphi_1^2(t) + \frac{1}{2} B_2 \varphi_2^2(t) + \frac{1}{2} B_3 \varphi_3^2(t) \right) dt \qquad (6)$$

with $B_1, B_2,$ dan B_3 respectively are the weight constants of the control variables in the form of costs for health education (φ_1), vaccination (φ_2), and isolation (φ_3). T represents the end time of the observation.

Our primary focus is on identifying the optimal control $(\varphi_1^*, \varphi_2^*, \varphi_3^*)$ such that

$$J(\varphi_1^*, \varphi_2^*, \varphi_3^*) = \min_{\varphi_1, \varphi_2, \varphi_3 \in \phi} J(\varphi_1, \varphi_2, \varphi_3)$$

where $\phi = \{(\varphi_1, \varphi_2, \varphi_3) | \varphi_i(t)$ is Lebesque measurable on $[0,1], (i = 1,2,3)\}$. Based on system (3) and index performance in (6), a Hamiltonian function can be formed as:

$$\mathcal{H} = \mathcal{H}\big(x(t), \varphi(t), \lambda(t)\big) = I_1 + I_2 + \tfrac{1}{2}B_1\varphi_1^2(t) + \tfrac{1}{2}B_2\varphi_2^2(t) + \tfrac{1}{2}B_3\varphi_3^2(t) + \lambda_1\Big(\Lambda - (1 - \varphi_1(t))\tfrac{\beta_1 SI}{N} - (1 - \varphi_1(t))\tfrac{\beta_1 SI_2}{N} - (1 + \varphi_2(t))\sigma S - \mu S\Big) + \lambda_2\Big((1 - \varphi_1(t))\tfrac{\beta_1 SI_1}{N} + (1 - \varphi_1)\tfrac{\beta_1 \omega_1 VI_1}{N} - \alpha_1 E_1 - \mu E_1\Big) + \lambda_4\Big((1 + \varphi_2(t))\sigma S - (1 - \varphi_1(t))\tfrac{\beta_1 \omega_1 VI_1}{N} - (1 - \varphi_1(t))\tfrac{\beta_2 \omega_2 VI_2}{N} - \mu V\Big) + \lambda_5(\alpha_1 E_1 - \varphi_3(t)I_1 - \gamma_1 I_2 - \mu I_1) + \lambda_6(\alpha_2 E_2 - \varphi_3(t)I_2 - \gamma_2 I_2 - \mu I_2) + \lambda_7(\varphi_3(t)I_1 + \varphi_3(t)I_2 - \gamma_3 H - \mu H) + \lambda_8(\gamma_1 I_1 + \gamma_2 I_2 + \gamma_3 Q - \mu R).$$

where $x(t) = (S(t), E_1(t), E_2(t), V(t), I_1(t), I_2(t), Q(t), R(t))$ is state system (3) and $\lambda_i, i = 1,2,3,4,5,6,7,8$ are the adjoint variables or costate variable.

Theorem 1. Suppose given the solutions $S(t), E_1(t), E_2(t), V(t), I_1(t), I_2(t), Q(t), R(t)$ of the state system (3) and optimal control pairs $(\varphi_1^*, \varphi_2^*, \varphi_3^*)$, there exist costate variables $\lambda_i, i = 1,2,3,4,5,6,7,8$, which fulfill the following adjoint system:

$$\dot{\lambda}_1 = (\lambda_1 - \lambda_2)\tfrac{\beta_1 I_1}{N}\Big(1 - \tfrac{S}{N}\Big)(1 - \varphi_1) + (\lambda_1 - \lambda_3)\tfrac{\beta_2 I_2}{N}\Big(1 - \tfrac{S}{N}\Big)(1 - \varphi_1) + (\lambda_1 - \lambda_4)(1 + \varphi_2)\alpha + \mu\lambda_1$$

$$\dot{\lambda}_2 = (\alpha_1 + \mu)\lambda_2 - \alpha_1\lambda_5$$

$$\dot{\lambda}_3 = (\alpha_2 + \mu)\lambda_3 - \alpha_2\lambda_6$$

$$\dot{\lambda}_4 = (\lambda_4 - \lambda_2)\tfrac{\beta_1 \delta_1 I_1}{N}\Big(1 - \tfrac{V}{N}\Big)(1 - \varphi_1) + (\lambda_4 - \lambda_3)\tfrac{\beta_2 \omega_2 I_2}{N}\Big(1 - \tfrac{V}{N}\Big)(1 - \varphi_1) + \mu\lambda_4$$

$$\dot{\lambda}_5 = -1 + (\lambda_1 - \lambda_2)\tfrac{\beta_1 S}{N}\Big(1 - \tfrac{I_1}{N}\Big)(1 - \varphi_1) + (\lambda_4 - \lambda_2)\tfrac{\beta_1 \omega_1 V}{N}\Big(1 - \tfrac{I_1}{N}\Big)(1 - \varphi_1) + \lambda_5(\varphi_3 + \gamma_1 + \mu) - \varphi_3\lambda_7 - \gamma_1\lambda_8$$

$$\dot{\lambda}_6 = -1 + (\lambda_1 - \lambda_3)\tfrac{\beta_2 S}{N}\Big(1 - \tfrac{I_2}{N}\Big)(1 - \varphi_1) + (\lambda_4 - \lambda_3)\tfrac{\beta_2 \omega_2 V}{N}\Big(1 - \tfrac{I_2}{N}\Big)(1 - \varphi_1) + \lambda_6(\varphi_3 + \gamma_2 + \mu) - \varphi_3\lambda_7 - \gamma_2\lambda_8$$

$$\dot{\lambda}_7 = \lambda_7(\gamma_3 + \mu) - \gamma_3\lambda_8$$

$$\dot{\lambda}_8 = \mu\lambda_8.$$

The costate equation system related to the optimal controls $(\varphi_1^*, \varphi_2^*,, \varphi_3^*) \in \phi$ and satisfying the transversality conditions $\lambda_i(T), i = 1,2,3,4,5,6,7,8$. As a result, the optimal controls are obtained as:

$$\varphi_1^* = \max\Big\{0, \min\Big\{1, \tfrac{1}{B_1}\Big((\lambda_2 - \lambda_1)\tfrac{\beta_1 SI_1}{N} + (\lambda_3 - \lambda_1)\tfrac{\beta_2 SI_2}{N} + (\lambda_2 - \lambda_4)\tfrac{\beta_1 \theta_1 VI_1}{N} + (\lambda_3 - \lambda_4)\tfrac{\beta_2 \theta_2 VI_2}{N}\Big)\Big\}\Big\}$$

$$\varphi_2^* = \max\Big\{0, \min\Big\{1, \tfrac{\sigma S(\lambda_1 - \lambda_4)}{B_2}\Big\}\Big\}$$

$$\varphi_3^* = \max\Big\{0, \min\Big\{1, \tfrac{(\lambda_5 - \lambda_7)I_1 + (\lambda_6 - \lambda_7)I_2}{B_3}\Big\}\Big\}.$$

3.4. Result of numerical simulation

In this subsection, we conduct numerical simulations on models both without and with control measures to illustrate the importance of implementing control strategies. Optimal control simulation is carried out using the forward-backward sweep algorithm. The parameter values used in the simulation are in Table 1. The weight values used are $B_1 = 10, B_2 = 20$, and $B_2 = 20$ and observation time $0 \le t \le 150$ days. In this paper, three control scenarios and seven control strategies are presented, encompassing a combination of health education $(\varphi_1(t))$, vaccination $(\varphi_2(t))$, and isolation measures $(\varphi_3(t))$.

- Scenario 1 consists of single controls, namely strategy 1 (health education control), strategy 2 (vaccination), and strategy 3 (isolation).

- Scenario 2 consists of double controls, there are strategy 4 (combined health education and vaccination control), strategy 5 (health education and isolation control), and strategy 6 (vaccination and isolation control).
- Scenario 3 is strategy 7, three control inputs of health education, vaccination, and isolation.

In Figure 3, control represents the change in control φ^* with time. Note that initially the optimal control φ_1^* (health education) takes a maximum value at $t \in [0.65]$, then at time $t \in [65,150]$ the optimal control value φ_1^* begins to decrease until on day 150 we obtain $\varphi\ \varphi_1^* = 0$. In optimal control φ_2^* (vaccination) takes a maximum value at $t \in [0.5]$, then at time $t \in [5,150]$ the optimal control value φ_2^* begins to decrease until day 150 we obtain $\varphi_2^* = 0$. Meanwhile, the optimal control φ_3^* (isolation) takes a maximum value at $t \in [0.95]$, then at time $t \in [95,150]$ the optimal control value φ_3^* begins to decrease until on day 150 we obtain $\varphi_3^* = 0$. This means that initially the control effort is carried out in full, then the control value decreases gradually until the end of the observation reaches zero.

To perform a comprehensive comparison of all available control strategies, an important step is to calculate the total number of infected individuals (TII) as well as the total cases averted (TCA) for each strategy. In other words, it is necessary to evaluate the effectiveness of each control strategy to assess its ability to reduce the number of people infected and the number of cases that can be prevented.

$$TII = \int_0^T \big(I_1(t) + I_2(t)\big)\, dt \text{ and } TCA = \int_0^T \Big(\hat{I}_1(t) + \hat{I}_2(t) - \big(I_1(t) + I_2(t)\big)\Big)\, dt,$$

where $\big(\hat{I}_1(t) + \hat{I}_2(t)\big)$ represents the number of infected individuals without control measures, $\big(I_1(t) + I_2(t)\big)$ denote the infected individuals with control strategy [4]. The outcomes of all computations are presented in Table 2.

In single input control scenarios, only isolation control showed a significant reduction in the number of infected individuals compared to health education and vaccination controls. This reduction occurred because, in model (3), isolation control is directly applied to already infected individuals, thus accelerating the decrease in the number of infected individuals as shown in Figure 4. In the double input control scenario in Figure 5, combining isolation control with other strategies, such as vaccination or health education, has a greater positive impact in reducing the number of infected individuals. Furthermore, the triple input control scenario showed better results compared to single and double input controls, indicating that the combination of these three strategies is more effective in controlling the spread of the virus. The implementation of the seventh strategy, which includes health education, vaccination, and isolation control, has proven successful in addressing the COVID-19 pandemic, reducing the spread of the virus and costs, as shown in Figure 6.
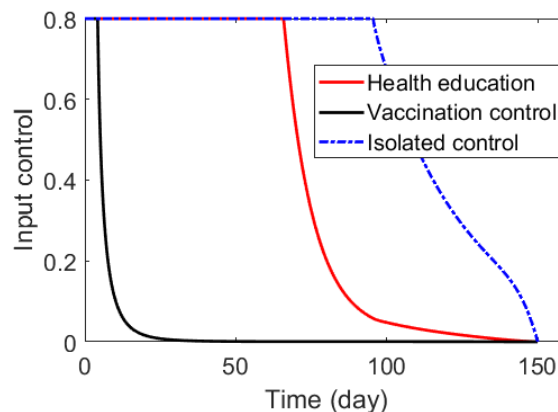

Figure 3. Optimal control by implementing health education, vaccination, and isolation controls

The combination of three strategies (health education, vaccination, and isolation) in dealing with the COVID-19 pandemic shows the highest effectiveness, with only 3,417,109 infected individuals and 88,752,048 cases averted, recording an infection averted ratio of 96.30% and a performance index of 3,417,510. This strategy is significantly superior compared to others. For instance, isolation control alone managed to reduce 88,596,984 cases with an averted ratio of 96.13%, while the combination of health education and isolation approaches a similar effectiveness with 96.28% cases averted. Meanwhile, the use of

vaccination alone was only able to avert 13.04% of infections. These results indicate that an integrated approach involving isolation, vaccination, and health education, when implemented together, provides the most comprehensive protection against the spread of COVID-19, underlining the importance of a multifaceted strategy in pandemic response.
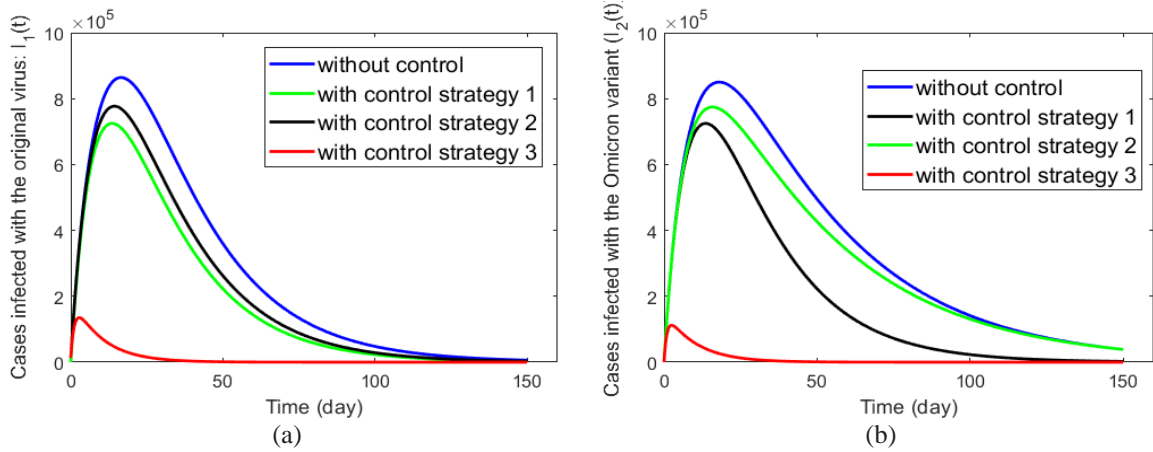

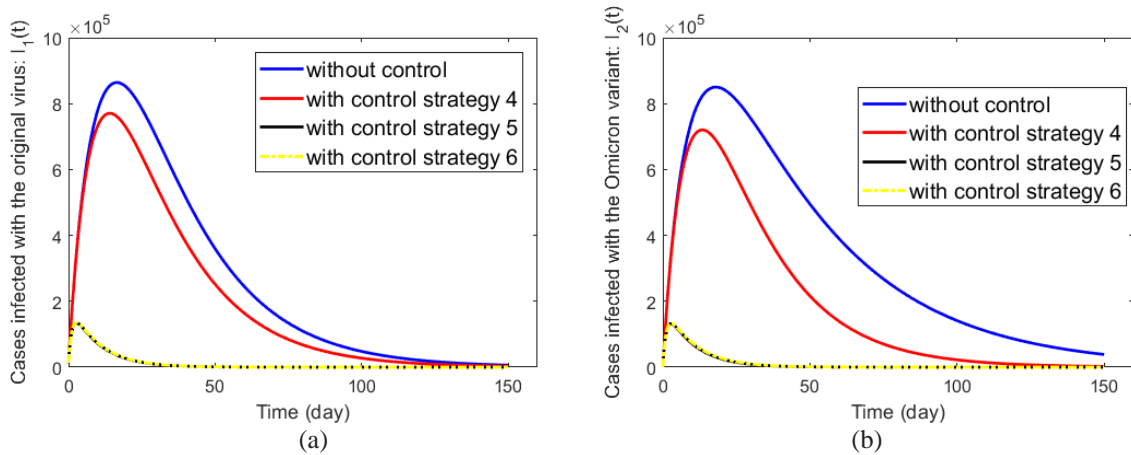Figure 4. Population dynamics $I_1(t)$ and $I_2(t)$ by implementing single control input

Figure 5. Population dynamics $I_1(t)$ and $I_2(t)$ by implementing double control input
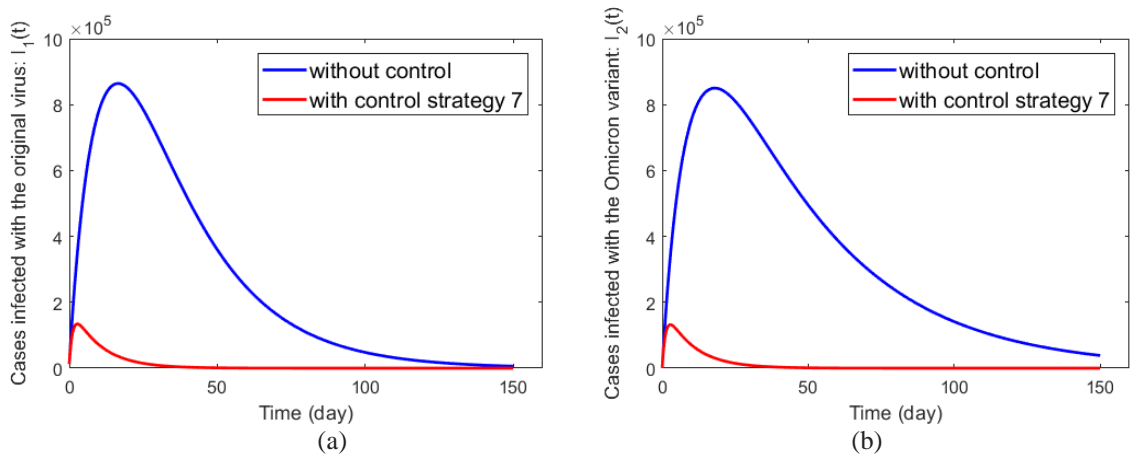
Figure 6. Population dynamics $I_1(t)$ and $I_2(t)$ by implementing three control input

Table 2. Comparison results of various strategies

Strategy control	Total infected individuals (TII)	Total cases averted (TCA)	Infection averted ratio	Index Performances
Without control	92,168,664	-	-	-
Health education control	62,226,360	29,941,797	32.49%	62,226,835
Vaccination control	880,149,964	12,018,700	13.04%	85,488,961
Isolation control	3,572,413	88,596,984	96.13%	3,572,413
Health education and vaccination control	60,031,120	32,137,037	34.87%	61,005,573
Health education and isolation control	3,423,317	88,744,840	96.28%	3,424,592
Vaccination and isolation	3,466,109	88,702,556	96.23%	3,528,234
Health education, vaccination, isolation control	3,416,109	88,752,048	96.30%	3,417,510

3.5. Discussion

Based on the results of this study, the combination of isolation, vaccination, and health education strategies in controlling the COVID-19 pandemic provides very high effectiveness, with an infection avoidance ratio reaching 96.30%. This significant reduction in cases supports findings by Ellwanger *et al.* [23], which emphasize that layered interventions can significantly enhance the control of infectious diseases. In this study, isolation as a direct intervention on infected individuals plays a vital role in accelerating case reduction, similar to conclusions drawn by Littlecott *et al.* [24] which show effective transmission reduction through strict isolation.

Although this study demonstrates the high effectiveness of a combination of health education, vaccination, and isolation strategies, the mere 13.04% effectiveness of vaccination alone in preventing infection highlights a significant gap compared to the 50% effectiveness reported by Okoli *et al.* [25] in preventing the spread of the influenza virus. This difference may be due to variability in immune response and the rapid mutation rate of COVID-19, which can reduce vaccine effectiveness. This underscores the need for ongoing adaptation in vaccine formulation and deployment strategies. As recommended by Vito *et al.* [26], adapting public health responses to the changing conditions of the pandemic is key to maintaining control over the spread of the virus.

The main purpose of this study is to test the effectiveness of combining various control strategies in addressing the COVID-19 pandemic and to demonstrate the importance of a multifaceted approach, which involves the simultaneous use of multiple strategies. These results are highly relevant to previous studies by Murni *et al.* [27], which documented that multifaceted intervention strategies are more likely to be successful in controlling the spread of complex diseases. Although this study provides valuable insights into the benefits of combination strategies, there are still unanswered questions related to the optimal implementation of these strategies on a larger scale. Therefore, future research needs to explore further how these elements can be effectively integrated into different public health policies, adjusting to population dynamics and epidemiological changes.

4. CONCLUSION

This study provides deep insights into the complexities of controlling the spread of COVID-19 amid the emergence of more infectious variants. Based on the data presented in table above and thorough discussions, it has been proven that the use of combined control strategies such as vaccination, health education, and isolation offer the most effective results in reducing the number of infected individuals and the transmission of the virus, as evidenced by the high infection averted ratio in these combined strategies. Strategies without control show high infection rates, underscoring the importance of proactive interventions. The use of health education and isolation, whether separately or in combination, shows a significant reduction in transmission, with the strategy that combines all three (health education, vaccination, and isolation) achieving the highest efficiency in controlling the virus spread. Additionally, the use of mathematical models enhanced with parameters estimated using the extended Kalman filter has provided strong predictive capabilities and supported evidence-based policy-making decisions. This underscores the importance of mathematical models in planning and evaluating responses to the pandemic.

In conclusion, the findings from this study highlight the importance of a holistic approach in managing the COVID-19 pandemic, where a combination of public health education, effective vaccination strategies, and strict isolation measures significantly contribute to reducing new cases. This is not only relevant for the scientific community but also for policymakers in designing and adjusting effective public health interventions for the future. This research also paves the way for further studies in optimizing disease control models, especially in the face of continuously emerging new variants. Thus, continued efforts in developing and implementing integrated and adaptive control strategies are crucial to addressing the

constantly changing dynamics of the pandemic, ensuring that the global community can respond quickly and efficiently to emerging health challenges.

REFERENCES

[1]   A. Li, Y. Wang, P. Cong, and X. Zou, "Re-examination of the impact of some non-pharmaceutical interventions and media coverage on the COVID-19 outbreak in Wuhan," *Infectious Disease Modelling*, vol. 6, pp. 975–987, 2021, doi: 10.1016/j.idm.2021.07.001.

[2]   A. Bolze *et al.*, "SARS-CoV-2 variant Delta rapidly displaced variant Alpha in the United States and led to higher viral loads," *Cell Reports Medicine*, vol. 3, no. 3, Mar. 2022, doi: 10.1016/j.xcrm.2022.100564.

[3]   F. Sheikhi, N. Yousefian, P. Tehranipoor, and Z. Kowsari, "Estimation of the basic reproduction number of Alpha and Delta variants of COVID-19 pandemic in Iran," *PLOS ONE*, vol. 17, no. 5, May 2022, doi: 10.1371/journal.pone.0265489.

[4]   T. Li and Y. Guo, "Modeling and optimal control of mutated COVID-19 (Delta strain) with imperfect vaccination," *Chaos, Solitons & Fractals*, vol. 156, Mar. 2022, doi: 10.1016/j.chaos.2022.111825.

[5]   H. Ri and X. Chen, "The updated strategy to overcome new challenge: Omicron variant (B.1.1.529) pandemic," *Clinical and Translational Discovery*, vol. 2, no. 1, Mar. 2022, doi: 10.1002/ctd2.28.

[6]   M. A. Khan and A. Atangana, "Mathematical modeling and analysis of COVID-19: A study of new variant Omicron," *Physica A: Statistical Mechanics and its Applications*, vol. 599, Aug. 2022, doi: 10.1016/j.physa.2022.127452.

[7]   R. Manjunath, S. L. Gaonkar, E. A. M. Saleh, and K. Husain, "A comprehensive review on COVID-19 Omicron (B.1.1.529) variant," *Saudi Journal of Biological Sciences*, vol. 29, no. 9, Sep. 2022, doi: 10.1016/j.sjbs.2022.103372.

[8]   M. A. Khan, K. Ali, E. Bonyah, K. O. Okosun, S. Islam, and A. Khan, "Mathematical modeling and stability analysis of pine wilt disease with optimal control," *Scientific Reports*, vol. 7, no. 1, Jun. 2017, doi: 10.1038/s41598-017-03179-w.

[9]   S. Annas, M. Isbar Pratama, M. Rifandi, W. Sanusi, and S. Side, "Stability analysis and numerical simulation of SEIR model for pandemic COVID-19 spread in Indonesia," *Chaos, Solitons & Fractals*, vol. 139, Oct. 2020, doi: 10.1016/j.chaos.2020.110072.

[10]   Y. Wang, P. Wang, S. Zhang, and H. Pan, "Uncertainty modeling of a modified SEIR epidemic model for COVID-19," *Biology*, vol. 11, no. 8, Aug. 2022, doi: 10.3390/biology11081157.

[11]   G.-Q. Sun *et al.*, "Transmission dynamics of COVID-19 in Wuhan, China: effects of lockdown and medical resources," *Nonlinear Dynamics*, vol. 101, no. 3, pp. 1981–1993, Jun. 2020, doi: 10.1007/s11071-020-05770-9.

[12]   T. Tottori and T. J. Kobayashi, "Forward-backward sweep method for the system of HJB-FP equations in memory-limited partially observable stochastic control," *Entropy*, vol. 25, no. 2, Jan. 2023, doi: 10.3390/e25020208.

[13]   C. E. Madubueze, S. Dachollom, and I. O. Onwubuya, "Controlling the spread of COVID-19: optimal control analysis," *Computational and Mathematical Methods in Medicine*, vol. 2020, pp. 1–14, Sep. 2020, doi: 10.1155/2020/6862516.

[14]   N. H. Sweilam, S. M. Al-Mekhlafi, A. O. Albalawi, and D. Baleanu, "On the optimal control of coronavirus (2019-nCov) mathematical model; a numerical approach," *Advances in Difference Equations*, vol. 2020, no. 1, 2020, doi: 10.1186/s13662-020-02982-6.

[15]   R. Djidjou-Demasse, Y. Michalakis, M. Choisy, M. T. Sofonea, and S. Alizon, "Optimal COVID-19 epidemic control until vaccine deployment," *medRxiv*, Apr. 2020, doi: 10.1101/2020.04.02.20049189.

[16]   D. N. Fisman, A. Amoako, and A. R. Tuite, "Impact of population mixing between vaccinated and unvaccinated subpopulations on infectious disease dynamics: implications for SARS-CoV-2 transmission," *Canadian Medical Association Journal*, vol. 194, no. 16, pp. 573–580, Apr. 2022, doi: 10.1503/cmaj.212105.

[17]   Y. R. Kim, Y.-J. Choi, and Y. Min, "A model of COVID-19 pandemic with vaccines and mutant viruses," *PLOS ONE*, vol. 17, no. 10, Oct. 2022, doi: 10.1371/journal.pone.0275851.

[18]   J. F. Lindahl and D. Grace, "The consequences of human actions on risks for infectious diseases: a review," *Infection Ecology & Epidemiology*, vol. 5, no. 1, Jan. 2015, doi: 10.3402/iee.v5.30048.

[19]   A. Hasan, "A nonlinear observer to estimate the effective reproduction number of infectious diseases," *Communication in Biomathematical Sciences*, vol. 4, no. 1, pp. 39–45, May 2021, doi: 10.5614/cbms.2021.4.1.4.

[20]   S. Lenhart and J. T. Workman, *Optimal control applied to biological models*. Chapman and Hall/CRC, 2007.

[21]   A. Hasan and Y. Nasution, "A compartmental epidemic model incorporating probable cases to model COVID-19 outbreak in regions with limited testing capacity," *ISA Transactions*, vol. 124, pp. 157–163, May 2022, doi: 10.1016/j.isatra.2021.01.029.

[22]   W.-Y. Chi *et al.*, "COVID-19 vaccine update: vaccine effectiveness, SARS-CoV-2 variants, boosters, adverse effects, and immune correlates of protection," *Journal of Biomedical Science*, vol. 29, no. 1, Oct. 2022, doi: 10.1186/s12929-022-00853-8.

[23]   J. H. Ellwanger, A. B. G. da Veiga, V. de L. Kaminski, J. M. Valverde-Villegas, A. W. Q. de Freitas, and J. A. B. Chies, "Control and prevention of infectious diseases from a One Health perspective," *Genetics and Molecular Biology*, vol. 44, 2021, doi: 10.1590/1678-4685-gmb-2020-0256.

[24]   H. Littlecott *et al.*, "Effectiveness of testing, contact tracing and isolation interventions among the general population on reducing transmission of SARS-CoV-2: a systematic review," *Philosophical Transactions of the Royal Society A: Mathematical, Physical and Engineering Sciences*, vol. 381, no. 2257, Aug. 2023, doi: 10.1098/rsta.2023.0131.

[25]   G. N. Okoli *et al.*, "Decline in seasonal influenza vaccine effectiveness with vaccination program maturation: a systematic review and meta-analysis," *Open Forum Infectious Diseases*, vol. 8, no. 3, Feb. 2021, doi: 10.1093/ofid/ofab069.

[26]   D. Vito, P. Lauriola, and C. D'Apice, "The COVID-19 pandemic: reshaping public health policy response envisioning health as a common good," *International Journal of Environmental Research and Public Health*, vol. 19, no. 16, Aug. 2022, doi: 10.3390/ijerph19169985.

[27]   I. K. Murni *et al.*, "Multifaceted interventions for healthcare-associated infections and rational use of antibiotics in a low-to-middle-income country: Can they be sustained?," *PLOS ONE*, vol. 15, no. 6, Jun. 2020, doi: 10.1371/journal.pone.0234233.

BIOGRAPHIES OF AUTHORS

Dewi Suhika ID SC ○ currently completing her doctoral studies at Institut Teknologi Bandung. She is current lecturer and researcher member in Department of Mathematics, Institut Teknologi Sumatera. Her research interests include control, optimization, and mathematical models in epidemiology. She can be contacted at email: dewi.suhika@ma.itera.ac.id or 30120006@mahasiswa.itb.ac.id.

Roberd Saragih ID SC ○ received his B.S. degree in mathematics and a Magister's degree in instrumentation and control from Institut Teknologi Bandung, Indonesia, in 1986, and 1993, respectively. He received a Ph.D. degree in mechanical engineering from Keio University, Japan, in 1998. From 1989, he joined the Department of Mathematics, Institut Teknologi Bandung, where he is currently a professor of mathematics. His general area of interest is robust control, system theory, and stochastic control. He can be contacted at email: roberd@math.itb.ac.id.

Dewi Handayani ID SC ○ received the B.S. degree, magister degree, and doctor degree in mathematics from Bandung Institute of Technology. She is current lecturer and researcher member in Department of Mathematics at Institut Teknologi Bandung. Her general area of interest is biomathematical model, robust control, stochastic control, and system theory. She can be contacted at email: dewi.handayani@math.itb.ac.id.

Mochamad Apri ID SC ○ received his B.S. degree in mathematics in mathematics from Institut Teknologi Bandung, Indonesia. He received master degree from Universitat Kaiserlautern, Germany. He received a Ph.D. degree from Wageningen University, Netherlands. He joined the Department of Mathematics, Institut Teknologi Bandung, where he is current lecturer and researcher member in Department of Mathematics at Institut Teknologi Bandung. His general area of interest is system biology and mathematical modeling. He can be contacted at email: m.apri@math.itb.ac.id.